Charge transport through a molecule driven by a high-frequency field

Sigmund Kohler, Sébastien Camalet, Michael Strass, Jörg Lehmann, Gert-Ludwig Ingold, Peter Hänggi

Angaben zur Veröffentlichung / Publication details:

Kohler, Sigmund, Sébastien Camalet, Michael Strass, Jörg Lehmann, Gert-Ludwig Ingold, and Peter Hänggi. 2004. "Charge transport through a molecule driven by a high-frequency field." *Chemical Physics* 296 (2-3): 243–49. https://doi.org/10.1016/j.chemphys.2003.09.023.

Charge transport through a molecule driven by a high-frequency field ☆

Sigmund Kohler, Sébastien Camalet [1], Michael Strass, Jörg Lehmann, Gert-Ludwig Ingold *, Peter Hänggi

Institut für Physik, Universität Augsburg, Universitätsstraße 1, D-86135 Augsburg, Germany

1. Introduction

The development of techniques to contact molecules and to drive a current through them [1–3] has opened the new and promising field of molecular electronics [4,5]. In order to construct useful devices, however, it is not sufficient to have a current flowing through a molecule but one also needs to have the ability to control this current. This can be achieved in principle by means of the so-called single electron transistor setup where a gate electrode is placed close to the molecule. Applying a gate voltage then allows to influence the current across the molecule. In more complex circuits, the need for a large number of contacts or electrodes close to the molecule may constitute a major obstacle. In fact, already the implementation of a single gate electrode which creates a sufficiently strong field at the molecule is a demanding task [6–8]. Therefore, other means of controlling the current through a nanosystem should be explored. One possibility is to replace the static field of a gate electrode by a suitable external ac field. Recent theoretical work [9] has demonstrated that, by using a coherent monochromatic field, one should indeed be able to control the electrical current flowing through a nanosystem connected to several leads. In an extension [10] of this work, it was demonstrated that even the noise level can be suppressed by an appropriate driving field.

In the present paper, we represent the molecule by a two-site system under the influence of an external high-frequency field and coupled to leads. Such a model is not limited to describe electrical transport through molecules but may also be applied to other situations like coherently coupled quantum dot systems [11] irradiated by microwaves.

In [10], a Floquet approach was employed to derive exact expressions for both, the current and the associated noise for the transport through a non-interacting nanosystem in the presence of an arbitrary time-periodic field. A study of the Fano factor [12], i.e. the ratio between

☆ Dedicated to the 60th birthday of Ulrich Weiss.

* Corresponding author. Fax: +49-821-598-3222.

E-mail address: gert.ingold@physik.uni-augsburg.de (G.-L. Ingold).

[1] Present and permanent address: Laboratoire de Physique, Ecole Normale Supérieure, 69364 Lyon Cedex 07, France.

noise and current, revealed a suppression at certain values of driving amplitude and frequency. To achieve a better physical understanding of this phenomenon, we here consider the problem within the high-frequency regime, which allows us to approximate the driven system by a static one with renormalised parameters. The structure observed for the Fano factor can then be understood in terms of three different scenarios. For small effective intramolecular hopping matrix elements, the system itself acts as a bottleneck, while in the opposite limit, the two contacts form a two-barrier setup. In between, when the hopping matrix element is of the order of the system–lead coupling strength, the barriers effectively disappear, leading to a suppression of the Fano factor.

In the next section, we introduce our model, consisting of two sites subject to an external oscillating field and coupled to two leads. We then discuss this model in the static case, deriving explicit expressions for both the current and its noise. In Section 4, expressions for the effective hopping matrix element and the electron distribution functions in the leads are determined within the high-frequency approximation. These results are used in Section 5 to compute current, noise and the corresponding Fano factor. A comparison with results based on the exact expressions of [10] demonstrates the validity of the high-frequency approximation for not too low frequencies. This allows a physical interpretation of the observed features in terms of a static model.

2. The model

In the following, we consider the setup depicted in Fig. 1, which we describe by the time-dependent Hamiltonian

$$H(t) = H_{\text{system}}(t) + H_{\text{leads}} + H_{\text{contacts}}. \tag{1}$$

The first term on the right-hand side

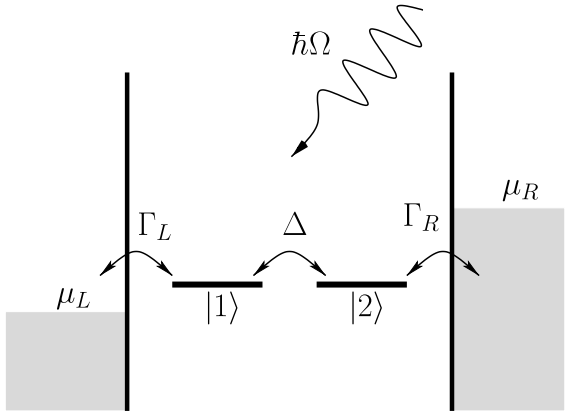

Fig. 1. Level structure of the nanoscale conductor with two sites. Each site is coupled to the respective lead with chemical potentials μ_{L} and $\mu_{\text{R}} = \mu_{\text{L}} + eV$.

$$H_{\text{system}}(t) = -\Delta(c_1^\dagger c_2 + c_2^\dagger c_1) + \frac{A}{2}(c_1^\dagger c_1 - c_2^\dagger c_2)\cos(\Omega t) \tag{2}$$

represents the driven two-site system, where electron–electron and electron–phonon interactions have been disregarded. The fermion operators c_n and $c_n^\dagger$, $n = 1, 2$, annihilate and create, respectively, an electron at site n. Both sites are coupled by a hopping matrix element Δ. The applied ac field with frequency $\Omega = 2\pi/\mathscr{T}$ results in a dipole force given by the second term in the Hamiltonian (2). The amplitude A is proportional to the component of the electric field strength parallel to the system axis.

The electrons in the leads are described by the Hamiltonian

$$H_{\text{leads}} = \sum_q (\epsilon_{\text{L}q} c_{\text{L}q}^\dagger c_{\text{L}q} + \epsilon_{\text{R}q} c_{\text{R}q}^\dagger c_{\text{R}q}), \tag{3}$$

where $c_{\text{L}q}^\dagger$ ($c_{\text{R}q}^\dagger$) creates a spinless electron in the left (right) lead with momentum q. The electron distribution in the leads is assumed to be grand canonical with inverse temperature $\beta = 1/k_{\text{B}}T$ and electro-chemical potential $\mu_{\text{L/R}}$. An applied voltage V corresponds to $\mu_{\text{R}} - \mu_{\text{L}} = eV$, where $-e$ is the electron charge.

The tunnelling Hamiltonian

$$H_{\text{contacts}} = \sum_q \left(V_{\text{L}q} c_{\text{L}q}^\dagger c_1 + V_{\text{R}q} c_{\text{R}q}^\dagger c_2 \right) + \text{h.c.} \tag{4}$$

establishes the contact between the sites and the leads, as sketched in Fig. 1. The system–lead coupling is specified by the spectral density

$$\Gamma_\ell(E) = 2\pi \sum_q |V_{\ell q}|^2 \delta(E - \epsilon_{\ell q}) \tag{5}$$

with $\ell = \text{L}, \text{R}$. Below, we shall assume within a so-called wide-band limit that these spectral densities are energy independent, $\Gamma_\ell(E) = \Gamma_\ell$.

3. Transport through a static two-site system

We start by deriving expressions for current and noise for a static two-site system coupled to two leads, setting $A = 0$ in the Hamiltonian (2). Solving the Heisenberg equations of motion for the lead operators, we obtain

$$c_{\text{L}q}(t) = c_{\text{L}q}(t_0) \mathrm{e}^{-\mathrm{i}\epsilon_{\text{L}q}(t-t_0)/\hbar} - \frac{\mathrm{i}V_{\text{L}q}}{\hbar} \int_{t_0}^{t} \mathrm{d}t' \, \mathrm{e}^{-\mathrm{i}\epsilon_{\text{L}q}(t-t')/\hbar} c_1(t') \tag{6}$$

and a corresponding expression for $c_{\text{R}q}(t)$ with L replaced by R and c_1 by c_2. Inserting (6) into the Heisenberg equations of motion of the two-site system and exploiting the wide-band limit, one arrives at

$$\dot{c}_1 = \frac{\mathrm{i}}{\hbar} \Delta \, c_2 - \frac{\Gamma_{\text{L}}}{2\hbar} c_1 + \xi_{\text{L}}(t), \tag{7}$$

$$\dot{c}_2 = \frac{\mathrm{i}}{\hbar}\Delta c_1 - \frac{\Gamma_\mathrm{R}}{2\hbar}c_2 + \xi_\mathrm{R}(t). \tag{8}$$

For a grand canonical ensemble, the operator-valued Gaussian noise

$$\xi_\ell(t) = -\frac{\mathrm{i}}{\hbar}\sum_q V_{\ell q}^* \exp\left[-\frac{\mathrm{i}}{\hbar}\epsilon_{\ell q}(t-t_0)\right] c_{\ell q}(t_0) \tag{9}$$

obeys

$$\langle \xi_\ell(t)\rangle = 0, \tag{10}$$

$$\langle \xi_\ell^\dagger(t)\xi_{\ell'}(t')\rangle = \delta_{\ell\ell'}\frac{\Gamma_\ell}{2\pi\hbar^2}\int \mathrm{d}\epsilon\, \mathrm{e}^{\mathrm{i}\epsilon(t-t')/\hbar} f_\ell(\epsilon), \tag{11}$$

where $f_\ell(\epsilon) = \{1+\exp[\beta(\epsilon-\mu_\ell)]\}^{-1}$ denotes the Fermi function with chemical potential μ_ℓ, $\ell = \mathrm{L},\mathrm{R}$. In the asymptotic limit $t_0 \to -\infty$, the solutions of Eqs. (7) and (8) read with $n = 1, 2$:

$$c_n(t) = \int_0^\infty \mathrm{d}\tau\, \{G_{n1}(\tau)\xi_\mathrm{L}(t-\tau) + G_{n2}(\tau)\xi_\mathrm{R}(t-\tau)\}. \tag{12}$$

In the wide-band limit and for equal system–lead coupling, $\Gamma_\ell = \Gamma$, the propagator is given by

$$G(\tau) = \mathrm{e}^{-\Gamma\tau/2\hbar}\begin{pmatrix} \cos(\Delta\tau/\hbar) & \mathrm{i}\sin(\Delta\tau/\hbar) \\ \mathrm{i}\sin(\Delta\tau/\hbar) & \cos(\Delta\tau/\hbar)\end{pmatrix}\Theta(\tau), \tag{13}$$

where $\Theta(\tau)$ is the Heaviside step function.

The operators corresponding to the currents across the contacts $\ell = \mathrm{L},\mathrm{R}$ are given by the negative time derivative of the electron number $N_\ell = \sum_q c_{\ell q}^\dagger c_{\ell q}$ in the respective lead, multiplied by the electron charge $-e$. For the current through the left contact one finds

$$\begin{aligned} I_\mathrm{L}(t) &= \frac{\mathrm{i}e}{\hbar}\sum_q \left(V_{\mathrm{L}q}^* c_1^\dagger c_{\mathrm{L}q} - \mathrm{h.c.}\right) \\ &= \frac{e}{\hbar}\Gamma_\mathrm{L} c_1^\dagger(t)c_1(t) - e\left\{c_1^\dagger(t)\xi_\mathrm{L}(t) + \xi_\mathrm{L}^\dagger(t)c_1(t)\right\} \end{aligned} \tag{14}$$

with a corresponding expression for $I_\mathrm{R}(t)$. In the stationary limit, $t_0 \to -\infty$, the mean values of the currents across the two contacts agree and we obtain

$$I = \langle I_\mathrm{L}\rangle = \frac{e}{2\pi\hbar}\int \mathrm{d}E[f_\mathrm{R}(E) - f_\mathrm{L}(E)]T(E). \tag{15}$$

In the wide-band limit, the transmission $T(E)$ can be expressed in terms of $G_{12}(E)$, i.e. the Fourier transform of the propagator $G_{12}(\tau)$, as

$$T(E) = \Gamma_\mathrm{L}\Gamma_\mathrm{R}|G_{12}(E)|^2. \tag{16}$$

Making use of the propagator (13), the transmission for $\Gamma_\ell = \Gamma$ becomes [13]

$$T(E) = \frac{\Gamma^2\Delta^2}{|(E-\mathrm{i}\Gamma/2)^2 - \Delta^2|^2}. \tag{17}$$

The noise of the current through contact ℓ is given by the symmetric auto-correlation function of the current fluctuation operator $\Delta I_\ell(t) = I_\ell(t) - \langle I_\ell(t)\rangle$. It is possible to characterise the noise strength by its zero frequency component

$$S = \frac{1}{2}\int_{-\infty}^{+\infty} \mathrm{d}t\langle \Delta I_\ell(t)\Delta I_\ell(0) + \Delta I_\ell(0)\Delta I_\ell(t)\rangle, \tag{18}$$

which is independent of the contact ℓ. The quantity S may be expressed in terms of the transmission function $T(E)$ as [14]

$$\begin{aligned} S = \frac{e^2}{2\pi\hbar}\int \mathrm{d}E\{&T(E)[f_\mathrm{L}(E)[1-f_\mathrm{L}(E)] \\ &+ f_\mathrm{R}(E)[1-f_\mathrm{R}(E)]] \\ &+ T(E)[1-T(E)][f_\mathrm{R}(E) - f_\mathrm{L}(E)]^2\}. \end{aligned} \tag{19}$$

Two contributions to the zero-frequency noise S have to be distinguished: the first term is a temperature-dependent equilibrium noise according to the dissipation-fluctuation theorem [15] and dominates for $\beta eV \ll 1$. In contrast, for large voltages $\beta eV \gg 1$, the main contribution to the noise stems from the second term. This so-called shot noise has its physical origin in the discreteness of the charge carriers.

We now consider voltages larger than all other energy scales in the problem. As a consequence, the current noise will entirely be due to shot noise. Furthermore, in this limit, the results for current and noise will not depend on temperature. In expression (15) for the current, the difference of the Fermi distributions then practically equals one for energies where the transmission is non-vanishing. The current thus reads

$$I_\infty = \frac{e}{2\pi\hbar}T = \frac{e\Gamma}{2\hbar}\frac{\Delta^2}{\Delta^2 + (\Gamma/2)^2}, \tag{20}$$

where $T = \int \mathrm{d}E\, T(E)$ is the total transmission. With the same argument we find from (19) for the current noise

$$S_\infty = \frac{e^2\Gamma}{\hbar}\frac{2\Delta^2(\Gamma^4 - 2\Gamma^2\Delta^2 + 8\Delta^4)}{(4\Delta^2+\Gamma^2)^3}. \tag{21}$$

The relative noise strength can be characterised by the so-called Fano factor $F = S/eI$ [12] which, in the infinite voltage limit, becomes

$$F_\infty = \frac{\Gamma^4 - 2\Gamma^2\Delta^2 + 8\Delta^4}{(4\Delta^2+\Gamma^2)^2}. \tag{22}$$

In Fig. 2, the Fano factor F_∞ is depicted as a function of the ratio of the tunnelling matrix element Δ and the level width Γ. For weak system–lead coupling $\Gamma \ll \Delta$, the two contacts between the two-site system and the leads form the limiting step of the transport process. We effectively arrive at transport through a double-barrier system with a Fano factor $F_\infty = 1/2$ [16]. On the other hand, for $\Gamma \gg \Delta$ the two sites hybridise with the adjacent lead and effectively only a single barrier remains. This yields a Fano factor $F_\infty = 1$. At the crossover between these two regimes, the channel is optimally transparent and,

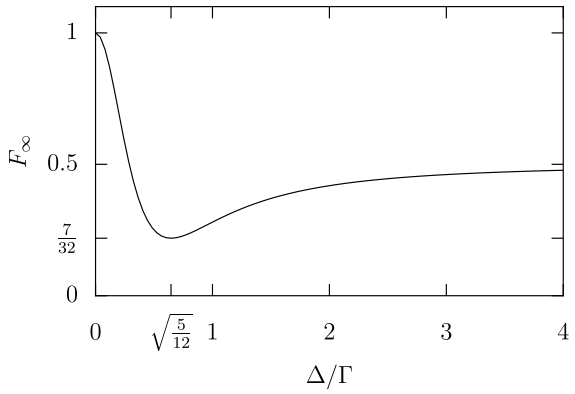

Fig. 2. Fano factor $F_\infty = S_\infty/eI_\infty$ as a function of Δ/Γ. For $\Delta \ll \Gamma$, the bottleneck of the transport is the tunnelling process between the two sites yielding a Fano factor $F_\infty = 1$. In the opposite limit $\Delta \gg \Gamma$, we obtain transport through a double-barrier structure with a corresponding Fano factor $F_\infty = 1/2$. In the intermediate regime the Fano factor assumes a minimum at the position indicated in the plot.

consequently, the Fano factor assumes a minimum. From expression (22), we find the optimal hopping matrix element $\Delta = \sqrt{5/12}\Gamma$ yielding a minimal Fano factor of $F_\infty = 7/32$. We remark that the minimum decreases further if the number of sites in the system is increased [10].

4. High-frequency approximation

Let us now turn back to the original time-dependent problem. We will compute within a high-frequency approximation [17] the current through this driven system and the corresponding current noise. Results valid for arbitrary driving amplitudes A can be obtained by the following procedure which is justified in the Appendix on the basis of Floquet theory.

First, we introduce the interaction picture with respect to the driving which for the problem at hand is obtained by means of the unitary transformation

$$U_0(t) = \exp\left(-\mathrm{i}\frac{A}{2\hbar\Omega}(c_1^\dagger c_1 - c_2^\dagger c_2)\sin(\Omega t)\right). \tag{23}$$

This yields the new system operators

$$\begin{aligned}\tilde{c}_{1,2}(t) &= U_0^\dagger(t) c_{1,2} U_0(t) \\ &= c_{1,2}\exp\left(\mp \mathrm{i}\frac{A}{2\hbar\Omega}\sin(\Omega t)\right),\end{aligned} \tag{24}$$

where the upper sign corresponds to site 1. To a good approximation, the dynamics can then be described by the time-averaged system Hamiltonian

$$\bar{H}_{\mathrm{system}} = -\Delta_{\mathrm{eff}}(c_1^\dagger c_2 + c_2^\dagger c_1). \tag{25}$$

Thus, within a high-frequency approximation, the driven two-site system acts as a static system with the effective hopping matrix element

$$\Delta_{\mathrm{eff}} = J_0(A/\hbar\Omega)\Delta, \tag{26}$$

where J_0 is the zeroth-order Bessel function of the first kind. The driving amplitude A and frequency Ω can now be chosen such that Δ_{eff} vanishes and consequently tunnelling between the two central sites then no longer occurs [17–19].

Proceeding as in Section 3, the influence of the leads after the transformation (23) can be described by fluctuation operators. For the left lead one finds

$$\begin{aligned}\eta_{\mathrm{L}}(t) = -\frac{\mathrm{i}}{\hbar}\sum_q V_{\mathrm{L}q}^* \exp\Bigg[-\frac{\mathrm{i}}{\hbar}\Bigg(&\epsilon_{\mathrm{L}q}(t-t_0) \\ &+ \frac{A}{2\Omega}\sin(\Omega t)\Bigg)\Bigg] c_{\mathrm{L}q}(t_0)\end{aligned} \tag{27}$$

with the correlation function

$$\begin{aligned}\langle \eta_{\mathrm{L}}^\dagger(t+\tau)\eta_{\mathrm{L}}(t)\rangle = \frac{\Gamma_{\mathrm{L}}}{2\pi\hbar^2}\int \mathrm{d}\epsilon \sum_{k,k'} \mathrm{e}^{\mathrm{i}\epsilon\tau/\hbar} f_{\mathrm{L}}(\epsilon + k\hbar\Omega) \\ \times J_k(A/2\hbar\Omega)J_{k'}(A/2\hbar\Omega)\mathrm{e}^{-\mathrm{i}(k-k')\Omega t}\end{aligned} \tag{28}$$

and corresponding expressions for the right lead. Since we are interested in the average current and the zero-frequency noise, i.e. low-frequency transport properties, we can neglect the $\mathscr{T}$-periodic contribution to the correlation function (28) and, thus, average its t-dependence over the driving period. Then, the correlation function assumes the form (11) like in the static case but with the Fermi function replaced by the effective distribution function

$$f_{\ell,\mathrm{eff}}(E) = \sum_{k=-\infty}^{\infty} J_k^2(A/2\hbar\Omega) f_\ell(E + k\hbar\Omega). \tag{29}$$

The different terms in this sum describe processes where an electron of energy E is transferred from lead ℓ to the system under absorption (emission) of $|k|$ photons for $k < 0$ ($k > 0$). These processes are weighted by the square of the kth-order Bessel function of the first kind.

Having approximated the originally time-dependent problem by a static one with an effective hopping matrix element and an effective distribution function, we can calculate the transmission, the current, and the zero frequency noise of the *driven* system with the formulae derived in Section 3 for a *static* situation.

In the limit of very large voltages and for energies where the transmission is nonvanishing, the effective distribution functions in the left and right lead become again zero or one, respectively. As a consequence, the time-averaged current and the zero-frequency noise are given by the expressions (20) and (21) with the replacement $\Delta \to \Delta_{\mathrm{eff}}$. We denote the current and the noise in this limit by $\bar{I}_\infty$ and $\bar{S}_\infty$, respectively. As pointed out above, there exist driving parameters where the effective hopping matrix element (26) vanishes. As a consequence, no current can flow through the system under these circumstances [9,10].

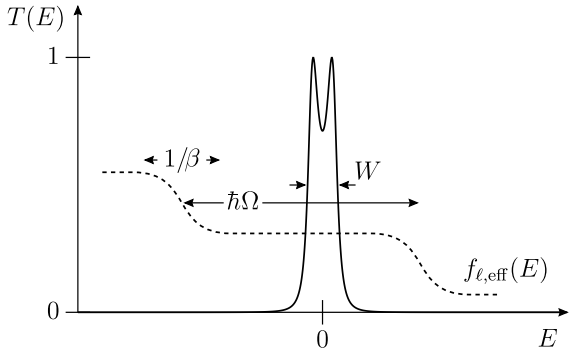

Fig. 3. Typical energy dependence of transmission $T(E)$ (solid line) and effective distribution function $f_{\ell,\mathrm{eff}}(E)$ (dashed line) which allows to replace the distribution function by (30) in the expressions for current and noise.

The case of a finite voltage requires a more detailed inspection of the distribution functions $f_{\ell,\mathrm{eff}}$ and the effective transmission $T(E)$ sketched in Fig. 3. In the high-frequency regime under study here, the width W of the transmission function is much smaller than $\hbar\Omega$. Furthermore, the effective distribution function $f_{\ell,\mathrm{eff}}$ is nearly constant for energies E separated by at least $1/\beta$ from the steps at $E = \mu_\ell + k\hbar\Omega$. Therefore, unless a step in $f_{\ell,\mathrm{eff}}$ occurs close to $E = 0$, the effective distribution functions in the current and noise expressions can be replaced by their value at $E = 0$, i.e.

$$f_{\ell,\mathrm{eff}} = \sum_{k<\mu_\ell/\hbar\Omega} J_k^2(A/2\hbar\Omega). \tag{30}$$

Thus, the time-averaged current and the zero-frequency noise are given by

$$\bar{I} = \bar{I}_\infty \quad J_0^2(A/2\hbar\Omega) + 2\sum_{k=1}^{K(V)} J_k^2(A/2\hbar\Omega)\Bigg), \tag{31}$$

$$\bar{S} = \frac{e}{2}\bar{I}_\infty + \quad J_0^2(A/2\hbar\Omega) + 2\sum_{k=1}^{K(V)} J_k^2(A/2\hbar\Omega)\Bigg)^2 \times \left(\bar{S}_\infty - \frac{e}{2}\bar{I}_\infty\right), \tag{32}$$

where $K(V)$ denotes the largest integer not exceeding $eV/2\hbar\Omega$. Note that the Fano factor $F = \bar{S}/e\bar{I}$ for fixed A/Ω reaches its minimal value in the infinite voltage limit. Since $J_k(x) \approx 0$ for $k > x$ and $\sum_k J_k^2(x) = 1$, the dc current and the zero frequency noise are well approximated for $A < eV$ by their asymptotic values for infinite voltage, $\bar{I} \approx \bar{I}_\infty$ and $\bar{S} \approx \bar{S}_\infty$. We remark that, in contrast to the static case, the result (32) contains contributions stemming from the first term in the noise expression (19) even in the zero-temperature limit.

5. Comparison with exact results

Figs. 4(b), (c) and (d) depict by solid lines the time-averaged current, the zero-frequency noise and the Fano factor at zero temperature obtained numerically within the Floquet approach of [10] for the relatively large voltage $V = 48\Delta/e$. This particular value of the voltage has been selected to avoid the chemical potentials to lie close to multiples of $\hbar\Omega$. A comparison of these numerically exact results for current and noise with the approximate expressions (31) and (32) depicted by dashed lines shows a good agreement for the parameters chosen. The agreement improves with increasing frequency: already for $\Omega = 10\Delta/\hbar$, it is found that the exact

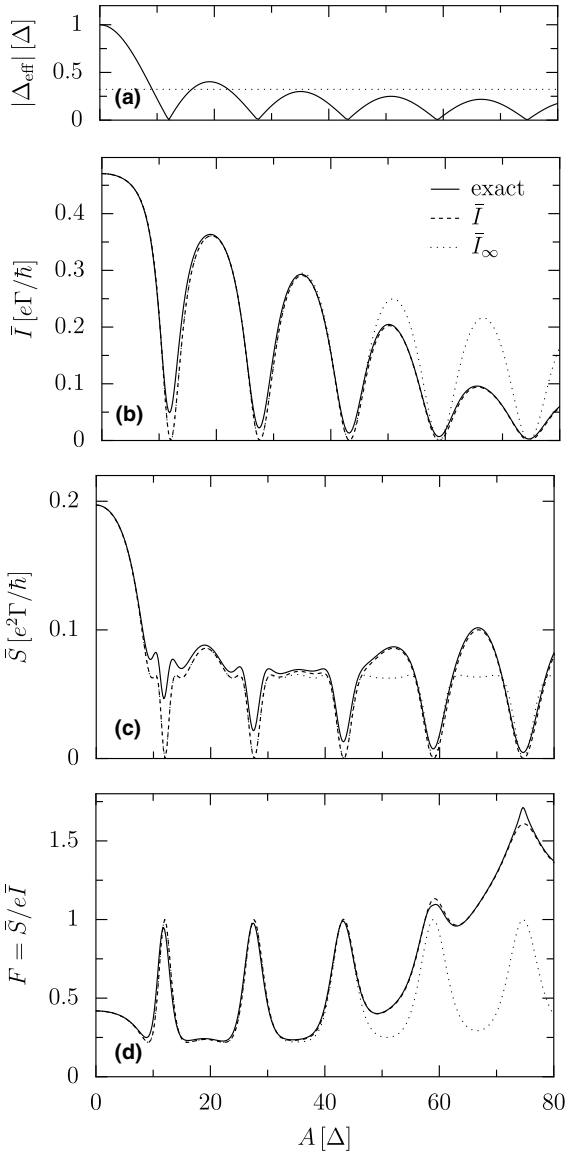

Fig. 4. (a) Effective hopping matrix element $|\Delta_{\mathrm{eff}}|$, (b) time-averaged current $\bar{I}$, (c) zero-frequency noise $\bar{S}$, and (d) Fano factor $F = \bar{S}/e\bar{I}$ as a function of the driving amplitude A. Shown are the numerically exact results (solid lines), the approximate results (31) and (32) for finite voltage (dashed lines), and the infinite voltage results (20) and (21) with Δ replaced by Δ_{eff} (dotted lines). The coupling strength is $\Gamma = 0.5\Delta$, the driving frequency is $\Omega = 5\Delta/\hbar$, and the voltage reads $V = 48\Delta/e$. The dotted line in (a) marks the value $\sqrt{5/12}\Gamma$ for which the Fano factor assumes its minimum.

and approximate results can practically no longer be distinguished.

The exact numerical results show strong suppressions of both, the current and the noise for certain driving amplitudes. This behavior can be explained within the high-frequency approximation presented in Section 4: Whenever the ratio $A/\hbar\Omega$ corresponds to a zero of the Bessel function J_0, the effective hopping matrix element Δ_{eff} vanishes (cf. Fig. 4(a)) and consequently the current and the noise become zero. Note that the exact result exhibits still a residual current and noise. The suppressions of the current and noise lead to peaks of the Fano factor F. For sufficiently small driving amplitudes, these peaks are accompanied by minima which correspond to $|\Delta_{\text{eff}}| \simeq \sqrt{5/12}\Gamma$ indicated by the dotted line in Fig. 4(a).

For driving amplitudes $A \lesssim eV$, the finite voltage results (31) and (32) for the current $\bar{I}$ and the noise $\bar{S}$ are well described by the results (20) and (21) for infinite voltage with Δ replaced by Δ_{eff}. In this regime, the Fano factor reaches maxima $F = 1$. In contrast, for larger driving amplitudes $A > eV$, we find a Fano factor larger than that predicted by (22), as discussed below (32). In particular, the Fano factor can assume values $F > 1$.

Finally, we consider in Fig. 5 the case of intermediate voltages such that $\Delta, \Gamma < eV < 2\hbar\Omega$. Then, only the zero photon channel contributes and hence the current $\bar{I} = \bar{I}_\infty J_0^2(A/2\hbar\Omega)$ is considerably lower than for large voltages. Now, in addition, a new type of suppression appears at twice the amplitude compared to the suppressions discussed above. The physical reason for this new kind of suppression lies in the fact that the effective distribution functions in the two leads are equal at the relevant energies and therefore no dc current can flow. Nevertheless, the noise remains finite and, consequently, the Fano factor diverges.

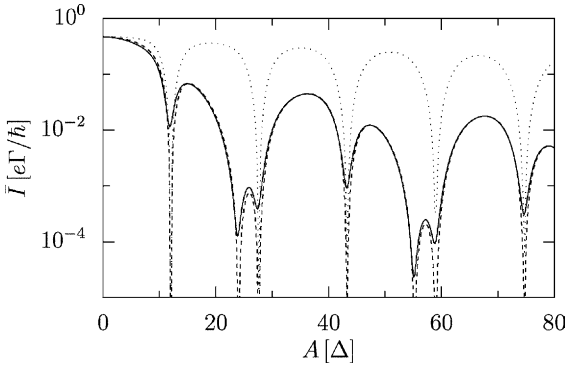

Fig. 5. Time-averaged current $\bar{I}$ as a function of the driving amplitude A. Shown are the numerically exact result (solid line), the approximate result (31) for finite voltage (dashed line) and the infinite voltage result (dotted line). The coupling strength is $\Gamma = 0.5\Delta$, the driving frequency is $\Omega = 5\Delta/\hbar$, and the voltage reads $V = 5\Delta/e$.

6. Conclusions

We have presented a high-frequency approximation for the charge transport through a driven two-site system. Within this scheme, the time-dependent Hamiltonian and the lead correlation functions are transformed to an appropriate interaction picture and subsequently time-averaged over the driving period. In the resulting equations, the hopping matrix element of the two-site system and the electron distributions of the attached leads are replaced by effective ones which depend on the driving parameters.

This static picture allows to gain profound physical insight into the structure present in current and noise as a function of the driving parameters. For small effective hopping matrix elements, the barrier between the two sites of the system dominates, leading to shot noise with $F = 1$. In the opposite limit, the contacts form a double-barrier system corresponding to a Fano factor $F = 1/2$. Between these two situations, effectively no barrier exists in the transport path and the Fano factor is further reduced to a minimal value of $F = 7/32$.

The results of this work demonstrate that the control of a current through a molecule by means of a time-periodic driving provides a viable alternative to the traditional single electron transistor setup based on a gate electrode. Our approach allows to minimise the number of electrodes close to the molecule. Furthermore, a suitable choice of the transistor's working point permits to operate in a low noise regime with a small Fano factor. These features inherent to the driven setup may prove useful for the development of novel molecular electronics devices.

Acknowledgements

The authors acknowledge financial support by a Marie Curie fellowship of the European community program IHP under contract No. HPMF-CT-2001-01416 (S.C.), by the Volkswagen-Stiftung under Grant No. I/77 217, and by the DFG through Graduiertenkolleg 283 and Sonderforschungsbereich 486.

Appendix A. Driven quantum systems in high-frequency approximation

In this Appendix, we review a common perturbative approach for the treatment of periodically time-dependent quantum systems and thereby justify the high-frequency approximation employed in Section 4.

A standard technique for the study of periodically time-dependent Hamiltonians $H(t) = H(t + \mathscr{T})$ is the so-called Floquet approach [20–22]. It starts out from the fact that a complete set of solutions of the corresponding

Schrödinger equation is of the form $|\psi_\alpha(t)\rangle = e^{-i\epsilon_\alpha t/\hbar}|\phi_\alpha(t)\rangle$ where the Floquet states $|\phi_\alpha(t)\rangle = |\phi_\alpha(t+\mathscr{T})\rangle$ obey the time-periodicity of the Hamiltonian. The Floquet states and the quasi-energies ϵ_α are eigenstates and eigenvalues, respectively, of the Hermitian operator $\mathscr{H} = H(t) - i\hbar d/dt$ defined in a Hilbert space extended by a periodic time coordinate. We emphasise that already the Floquet states from a single Brillouin zone $-\hbar\Omega/2 \leqslant \epsilon_\alpha < \hbar\Omega/2$ form a complete set of solutions. A Floquet ansatz essentially maps the time-dependent problem to an eigenvalue problem and, thus, it is possible to employ all approximation schemes known from time-independent quantum mechanics, in particular perturbative schemes for the computation of eigenstates.

Here, we consider the special case of a time-dependent Hamiltonian of the form

$$H = H_0 f(t) + H_1, \tag{A.1}$$

where $f(t)$ is a $\mathscr{T}$-periodic function with zero time-average. If $\hbar\Omega$ is much larger than all energy differences in the spectrum of H_1, the following Schrödinger perturbation theory can be employed for the computation of the Floquet states [20,21]: it is assumed that for H_0 all eigenstates $|\varphi_\alpha\rangle$ and eigenenergies E_α are known. Then, the unperturbed Floquet Hamiltonian $\mathscr{H}_0 = H_0 f(t) - i\hbar d/dt$ has the eigensolutions

$$|\phi_\alpha^k(t)\rangle = \exp\left(-\frac{i}{\hbar}E_\alpha F(t) + ik\Omega t\right)|\varphi_\alpha\rangle \tag{A.2}$$

with eigenvalue $k\hbar\Omega$. Here, $dF(t)/dt = f(t)$ and k is an arbitrary integer. Note that $F(t)$ satisfies the $\mathscr{T}$-periodicity of the field since the time average of $f(t)$ vanishes. Thus, k defines a degenerate subspace of the extended Hilbert space. In each degenerate subspace, the matrix elements of the perturbation read

$$(H_1)_{\alpha\beta} = \frac{1}{\mathscr{T}}\int_0^{\mathscr{T}} dt\, \langle\phi_\alpha^k(t)|H_1|\phi_\beta^k(t)\rangle. \tag{A.3}$$

Therefore, to first order in $H_1/\hbar\Omega$, the Floquet states and the quasienergies for the Hamiltonian (A.1) are obtained by diagonalising the perturbation matrix (A.3).

Following (A.2), the basis states $|\varphi_\alpha\rangle$ and $|\phi_\alpha^k(t)\rangle$ are related by the unitary transformation

$$U_0(t) = \exp\left(-\frac{i}{\hbar}H_0 F(t)\right) \tag{A.4}$$

as $\exp(-ik\Omega t)\,|\,\phi_\alpha^k(t)\rangle = U_0(t)\,|\,\varphi_\alpha\rangle$. For the Hamiltonian (2), (A.4) corresponds to the unitary transformation (23).

Within the regime of validity of the perturbative approach, the problem is therefore described by the static Hamiltonian

$$\bar{H}_1 = \frac{1}{\mathscr{T}}\int_0^{\mathscr{T}} dt\, U_0^\dagger(t) H_1 U_0(t). \tag{A.5}$$

Note that after the transformation with (A.4), the amplitude of the oscillating part of the new Hamiltonian $U_0^\dagger(t)H_1U_0(t)$ is no longer governed by H_0, but rather by H_1. Thus, a perturbative treatment of the oscillating part is (almost) independent of the original driving amplitude in H_0.

A particular example for a high-frequency approach along these lines is a particle moving in a one-dimensional continuous potential under the influence of a dipole field, i.e. $H_1 = p^2/2m + V(x)$ and $H_0 = \mu x$. Then, (A.4) constitutes a gauge transformation and results in a Hamiltonian which is again of the form (A.1). A second transformation of the type (A.4) yields a periodically accelerated potential and defines the so-called Kramers–Henneberger frame [23,24].

References

[1] M.A. Reed, C. Zhou, C.J. Muller, T.P. Burgin, J.M. Tour, Science 278 (1997) 252.
[2] X.D. Cui, A. Primak, X. Zarate, J. Tomfohr, O.F. Sankey, A.L. Moore, T.A. Moore, D. Gust, G. Harris, S.M. Lindsay, Science 294 (2001) 571.
[3] J. Reichert, R. Ochs, D. Beckmann, H.B. Weber, M. Mayor, H. von Löhneysen, Phys. Rev. Lett. 88 (2002) 176804.
[4] P. Hänggi, M. Ratner, S. Yaliraki (Eds.), Processes in Molecular Wires, Chem. Phys. 281 (2002) 111.
[5] A. Nitzan, M.A. Ratner, Science 300 (2003) 1384.
[6] W. Liang, M.P. Shores, M. Bockrath, J.R. Long, H. Park, Nature 417 (2002) 725.
[7] N.B. Zhitenev, H. Meng, Z. Bao, Phys. Rev. Lett. 88 (2002) 226801.
[8] J.-O. Lee, G. Lientschnig, F. Wiertz, M. Struijk, R.A.J. Janssen, R. Egberink, D.N. Reinhoudt, P. Hadley, C. Dekker, Nano Lett. 3 (2003) 113.
[9] J. Lehmann, S. Camalet, S. Kohler, P. Hänggi, Chem. Phys. Lett. 368 (2003) 282.
[10] S. Camalet, J. Lehmann, S. Kohler, P. Hänggi, Phys. Rev. Lett. 90 (2003) 210602.
[11] R.H. Blick, R.J. Haug, J. Weis, D. Pfannkuche, K. von Klitzing, K. Eberl, Phys. Rev. B 53 (1996) 7899.
[12] U. Fano, Phys. Rev. 72 (1947) 26.
[13] L.E. Hall, J.R. Reimers, N.S. Hush, K. Silverbrook, J. Chem. Phys. 112 (2000) 1510.
[14] Ya.M. Blanter, M. Büttiker, Phys. Rep. 336 (2000) 1.
[15] H.B. Callen, T.A. Welton, Phys. Rev. 83 (1951) 34.
[16] L.Y. Chen, C.S. Ting, Phys. Rev. B 43 (1991) 4534.
[17] F. Großmann, P. Jung, T. Dittrich, P. Hänggi, Z. Phys. B 84 (1991) 315.
[18] F. Großmann, P. Hänggi, Europhys. Lett. 18 (1992) 571.
[19] F. Grossmann, T. Dittrich, P. Jung, P. Hänggi, Phys. Rev. Lett. 67 (1991) 516.
[20] J.H. Shirley, Phys. Rev. 138 (1965) B979.
[21] H. Sambe, Phys. Rev. A 7 (1973) 2203.
[22] M. Grifoni, P. Hänggi, Phys. Rep. 304 (1998) 229.
[23] H.A. Kramers, Collected Scientific Papers, North-Holland, Amsterdam, 1956.
[24] W.C. Henneberger, Phys. Rev. Lett. 21 (1968) 838.